1972

# Laboratory Analysis Improves Crankshaft Design

L. L. Faulkner
*Ohio State University*

J. F. Hamilton
*Purdue University*

# LABORATORY ANALYSIS IMPROVES CRANKSHAFT DESIGN

Lynn L. Faulkner, Assistant Professor, Dept. of Mech. Engr.,
The Ohio State University, Columbus, Ohio.

James F. Hamilton, Professor of Mechanical Engineering,
The Ray W. Herrick Laboratories, Purdue University, Lafayette, Indiana

## ABSTRACT

This paper describes an experimental method of investigating stress concentrations in crankshafts of small reciprocating compressors, the object being to determine operating stresses for selection of materials, shapes of fillets, and geometry of oil holes and grooves. The procedure consisted of determining dynamic operating forces and, by means of experimental stress analysis techniques, stress values were obtained using an equivalent static measurement. An analytical method of calculating the operating stress due to an oil hole in the shaft was developed using results from the experimental stress analysis. With consideration of the oiling system and machining operations, the optimum relocation of the oil hole in a region of lower nominal stress was determined using the mathematical model.

## INTRODUCTION

It is not uncommon to extend mechanical devices to operating conditions beyond which the original design was intended. The result , in many cases, is the occurrence of component failures which previously were not encountered. A design re-analysis is usually necessary which in most cases is more elaborate than the original design of the component, but with the techniques presently available a more useful and optimal design can be achieved.

This particular investigation was undertaken to improve the design of a crankshaft from a single cylinder, hermetically-sealed refrigeration compressor. Because of the enclosed construction and the operating requirements, the methods of measuring forces during operation were not available a few decades ago and consequently the original designs were developed using broad guidelines and building a number of prototypes. When performance requirements necessitated increased loads, failures began to occur. Figure 1 shows the particular piston-slider-crank mechanism of interest, which is commonly referred to as a "ScotchYoke", and a typical failure. The hole visible at the broken section is part of the shaft oiling system and is easily seen to be a stress concentration area.

This work was sponsored by the White Corporation, Gibson Refrigerator Division, Greenville, Michigan.

## DETERMINATION OF FORCES

Before any analytical or experimental investigation of the crankshaft stresses could be made, it was necessary to have some understanding of the forces acting on the crankshaft during compressor operation. It was considered necessary to determine independently:

1. Pressure forces acting on the piston during the compressor cycle.
2. Inertia forces due to reciprocating motion of the piston and connecting mechanism.
3. Frictional forces of the slider-crank mechanism.

To determine the pressure forces acting on the piston during the cyclic operation, a crystal pressure transducer was mounted in the cylinder wall with a small opening to the clearance volume. A contact was attached to the crankshaft which completed an electrical circuit once every cycle and produced a signal as an indication of the top dead center position. Instrumentation cables were passed through the hermetic shell by means of seals which enabled the shell to be replaced and operated under normal R-12 pressure and temperature conditions.

While operating the compressor at normal conditions, the pressure signal from the transducer was amplified and displayed on an oscilloscope along with the reference timing pulse as shown in Figure 2. The upper trace represents the reference pulse. Notice that since the contact had finite area the response was not a sharp peak. When the compressor was assembled the contact was adjusted so that the midpoint of the trace, which is easily distinguishable, represents the top dead center position. The sweep rate of the oscilloscope was known as well as the speed of the compressor and thus by reference to the top dead center position, the pressures in the cylinder were known in relation to the angular rotation of the crankshaft. The pressure force component was plotted as a function of crank angle in Figure 3.

The forces were obtained from a dynamic analysis of the system. Figure 4 is a schematic of the piston-slider-crank mechanism with appropriate forces. The reciprocating inertia component, $F_2$, can be determined from

$$F_2 = \text{mass x acceleration} \quad (1)$$

$$F_2 = Me\omega^2 \cos \omega t \quad (2)$$

where

m = mass of piston + slider + pin

e = eccentricity of the crankshaft

$\omega$ = rotational speed of the compressor

t = time

The vertical component of the counterweight inertia was subtracted as a component force. It was necessary to include forces in this manner because the yoke was not completely balanced by the counterweight.

As written, the relation for $F_2$ can be related directly to the crank angle, $\theta$, with the top dead center position as reference. Using appropriate values for the above quantities, the inertia force was found to be

$$F_2 = -23.2 \cos \theta \text{ lbs} \quad (3)$$

This component was also plotted in Figure 3.

When determining friction forces there is usually some question concerning what coefficients of friction to use because of the dependence on surface finish, lubricant, temperature, and "run-in" of the bearing. In this application it was assumed that friction coefficients in the range of 0.01 to 0.05 would be appropriate for the sliding contact between the piston and slider. The maximum normal force acting on the slider surface is obtained from the maximum value of pressure and inertia forces which occurs at a crank angle of -40 degrees as indicated in Figure 3. As shown in Figure 4, the friction force, f, at the piston-slider interface is always in the horizontal direction and the sum of the pressure and major inertia force is always in the vertical direction.

The friction force was obtained by multiplying the normal force component, which in this case is the sum of the pressure and inertia forces, by a coefficient is usually small for well oiled bearings. It was shown by an order of magnitude procedure that the friction force could be neglected without introducing significant errors. The frictional forces at the piston-cylinder interface were also neglected. The total force acting on the crankshaft at the piston end was taken as the sum of the pressure and inertia forces as indicated in Figure 3.

## DETERMINING STRESSES

For a simply supported and loaded solid shaft the tensile and shearing stresses are given by

$$\sigma_x = \frac{MY}{I} \quad \tau_{xy} = \frac{Tr}{J} \quad \sigma_y = 0 \quad (6)$$

where

$\sigma_x, \sigma_y$ = x and y components of stress

$\tau_{xy}$ = shearing stress at radius r

M = bending moment

Y = distance from the neutral axis

T = torque

r = radius

J = polar moment of inertia

I = area moment of inertia

From the geometry of the crankshaft and from the observed failures it was clear that the maximum stress occurred at the oil hole when the piston was in the top dead center region. In this position the pressure forces are near the maximum values as indicated in Figure 3. When the pressure forces become small the oil hole location was such that it was in a region near the neutral axis and therefore the stress was small both at the oil hole and at other positions on the shaft because the load is reduced. It was evident that the stress at oil hole location as the oil hole rotates through 360° was of primary concern in the failure of the crankshaft.

From the geometry of the crankshaft the tensile and shearing stresses were obtained from equation 6. The following expressions were obtained for the stresses at the surface of the circular section at the oil hole location as the section rotated with the crankshaft.

$$\sigma_x = 17.1F(\theta) \sin (90^\circ - |\theta|)$$

$$\tau_{xy} = 1.515\, F(\theta) \quad (7)$$

where

$F(\theta)$ = total force from Figure 3

$\theta$ = crank angle from top dead center

Note that equation 7 is for a solid section and the influence of the oil hole has not been accounted for. The $\theta$ term is included because as the shaft rotates the oil hole changes location in relation to the bending axis. When $\theta = 90^\circ$ the oil hole would be located on the bending axis and be in a region of zero stress.

For a solid shaft the maximum stress at a particular location is called the principal stress and is a combination of the normal and shearing stresses given by:

$$\sigma_1 = \frac{\sigma_x+\sigma_y}{2} + \sqrt{\left(\frac{\sigma_x-\sigma_y}{2}\right)^2 + \tau_{xy}^{\ 2}} \qquad (8)$$

Noting that the maximum values of total force occur for values of $\theta$ of 40 degrees or less, it is easily verified that $\sigma_1$ will be in error by less than one percent if the shear stress is neglected. The principal stress of a solid cylindrical shaft without a stress concentration is represented by the relation,

$$\sigma_1 = 17.1\ F(\theta)\ \sin\ (90^\circ - |\theta|) \qquad (9)$$

The accuracy of this relation was verified experimentally and will be discussed in the next section.

In order to obtain the maximum stress which will occur for a section with a stress concentration it is desirable to determine a stress concentration factor, $K_t$, defined as

$$K_t = \frac{\sigma_{max}}{\sigma_1} = \frac{\text{maximum stress}}{\text{nominal stress}} \qquad (10)$$

and then

$$\sigma_{max} = K_t\ \ \sigma_1 \qquad (11)$$

Published values for $K_t$ are available for shafts with holes, but usually are obtained under idealized conditions. In this particular application the hole was near the fillet and the method of loading was not pure bending as is the case for most published values of shafts with holes. To obtain more accurate stress values, a value for the stress concentration factor for this particular condition was determined experimentally.

To allow the shaft to be coated with a strain indicating material and to provide support and loading the compressor casting was machined and a fixture was designed to bolt to the cylinder to allow force to be applied to the piston. A photograph of the test fixture is shown in Figure 5. The load was applied by turning the bolt against a crystal load cell which transmitted the force to the piston and to the crankshaft. The intent was to determine a stress concentration experimentally by applying a dynamically equivalent static load. Several castings were similarly modified to allow experimental values to be obtained for several crank positions.

To determine the accuracy of the experimental method, a shaft without a stress concentration in the form of the oil hole was coated with birefringent material and loaded statically with a force obtained from Figure 3, for various $\theta$ values. This experimental value was compared with the value obtained from equation 9. The experimental method gave stress values which differed from the calculated by 6 percent for a solid crankshaft without an oil hole.

Having established the validity of the experimental method, shafts with oil holes were coated and tested to determine the maximum stresses at the oil hole. A value for the stress concentration factor, $K_t$, was established as being equal to 3.6 and the maximum principal stress at the oil hole was found from equation 11 to be

$$\sigma_{max} = 61\ F(\theta)\ \sin\ (90^\circ - |\theta|) \qquad (12)$$

To allow for oil hole locations other than the existing location a factor $\alpha$ was introduced as follows:

$$\sigma_{max} = 61\ F(\theta)\ \sin\ (90^\circ - |\theta \pm \alpha|) \qquad (13)$$

The value of $\alpha$ then corresponds to the position of the oil hole when the crankshaft is in the $\theta = 0$ position.

## OIL HOLE LOCATION

Equation 13 above, along with the plot of force versus crank angle, allows numerical calculations to be made for stress values as functions of crank angle and load for any desired circumferential position of the oil hole. Several proposed oil hole relocations were considered and the stress values as a function of crank angle are shown plotted in Figure 6. From these curves a new oil hole location was selected with consideration for the oil pumpage requirements, and the machining operations required.

The hole could not be located where it would interfere with the bearing lubrication and existing manufacturing equipment and methods also limited some proposed positions.

The optimal location was selected at $78^\circ 45'$ leading angle from the existing oil hole position. A number of crankshafts were then machined with the new oil hole location, as shown in Figure 7, and were coated with birefringement material and tested using the static loading fixture as shown in Figure 5. The results of these tests are shown plotted with the dashed line on Figure 6.

## CONSLUSIONS

A dynamically equivalent static investigation is an adequate representation of crankshaft loading and the stress values did confirm that the original oil hole position had stress values above the endurance limit.

Although the stress values in Figure 6 may not be exact due to the order of magnitude analysis on the forces, the percentage decrease in stress can be used directly because identical testing conditions were used. In this particular case an acceptable solution was found from a rather simple static analysis and the amount of improvement could be established with some confidence within the limits established by the bearing lubrication and existing manufacturing methods.

REFERENCES


1. Dally, James W. and Riley, William F., "Experimental Stress Analysis", McGraw-Hill, 1965.

2. Faries, Virgil M., "Design of Machine Elements", The McMillan Company, 1955.

3. Hetenyi, M., "Handbook of Experimental Stress Analysis", John Wiley and Sons, 1950.

4. Lee, George H., "An Introduction to Experimental Stress Analysis", John Wiley and Sons, 1950.

5. Peterson, R. W., "Stress Concentration Design Factors", John Wiley and Sons, 1953.


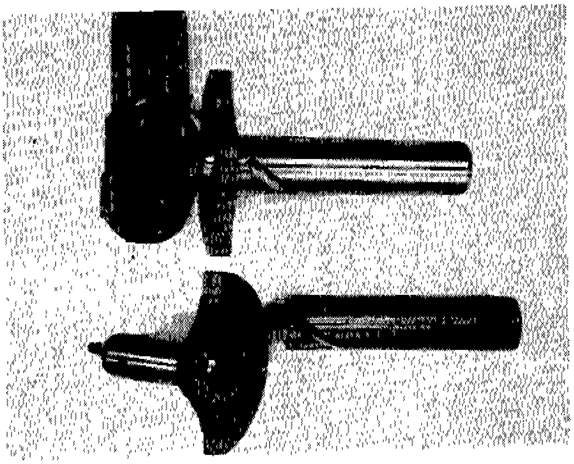

Figure 1. Scotch Yoke mechanism and a typical failure.

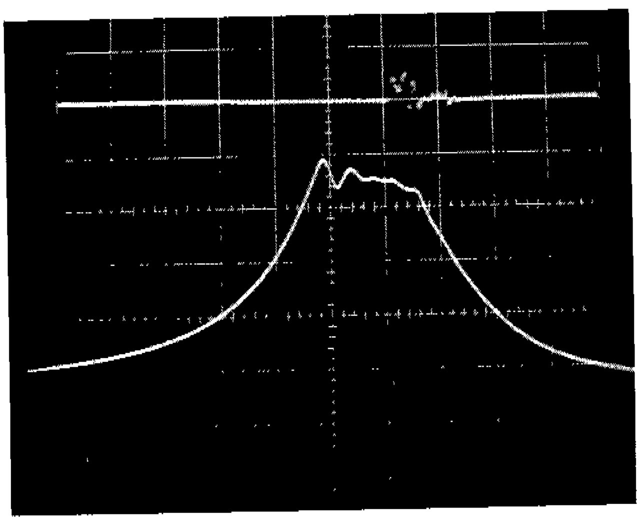

Figure 2. Pressure signal and top dead center reference.

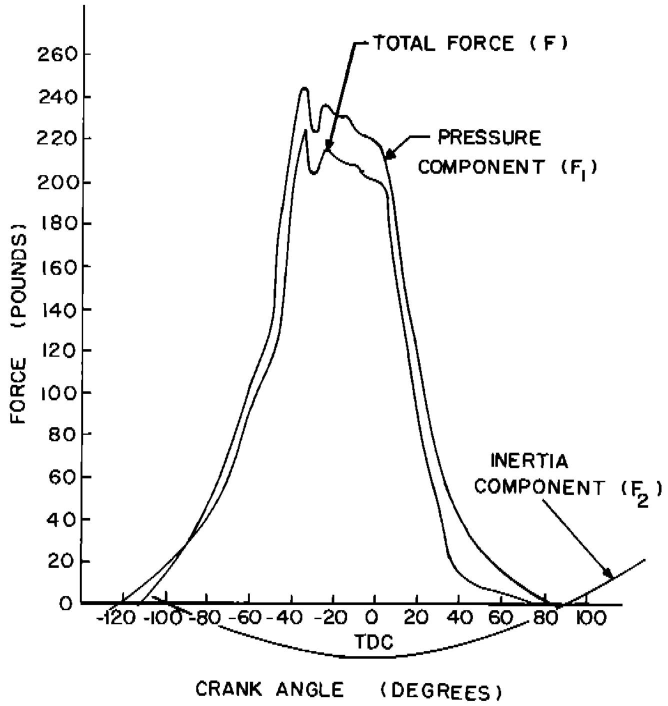


Figure 3. Forces versus crank angle.

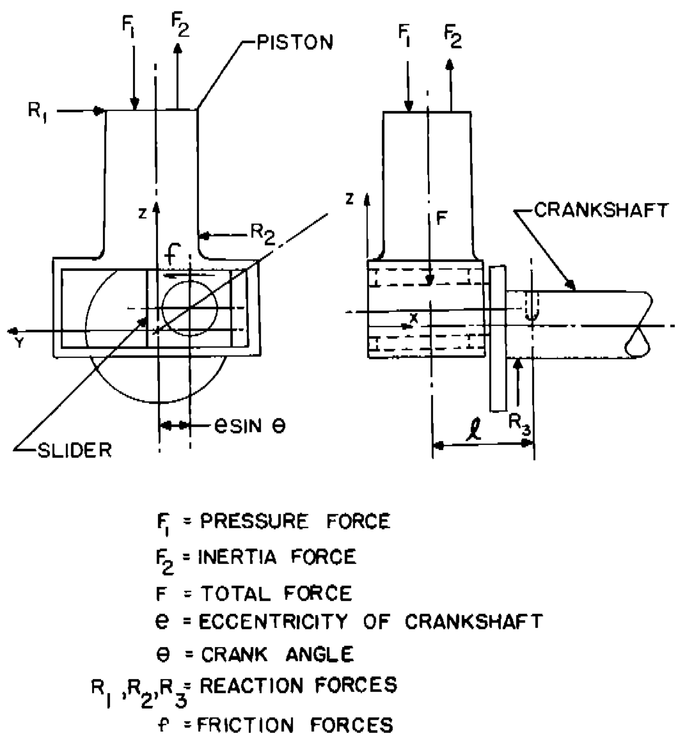


Figure 4. Piston-slider-crank mechanism.

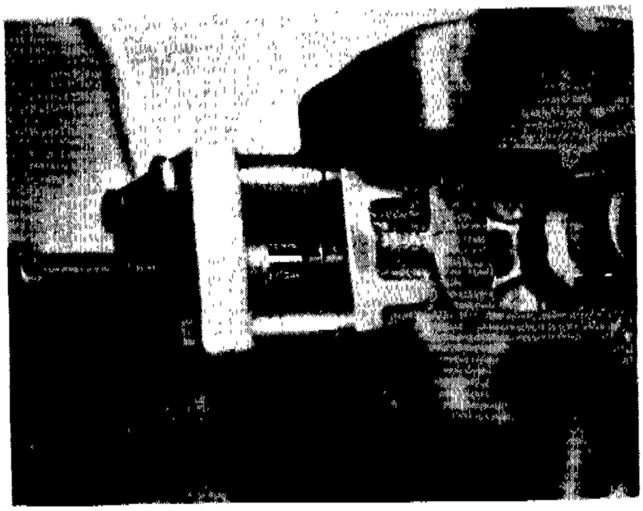

Figure 5. Static loading fixture with coated shaft exposed.

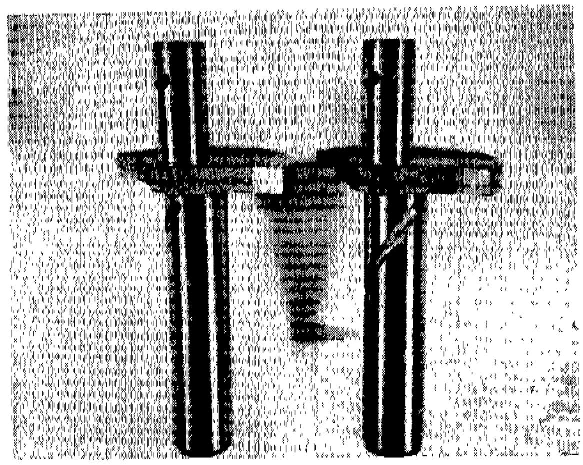

Figure 7. Comparison of original and redesigned crankshafts.

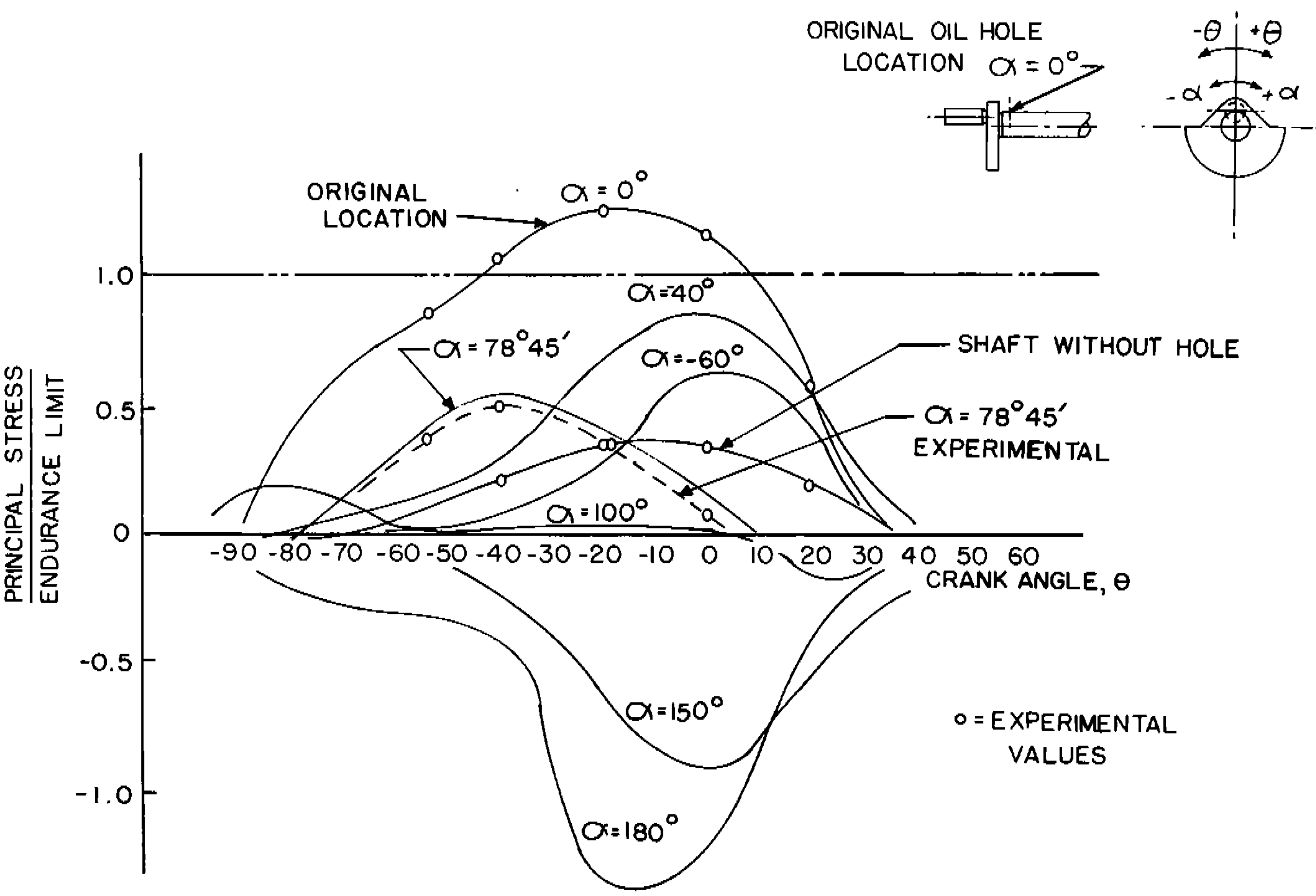


Figure 6. Maximum principal stress versus crank angle for various hole locations.